Advances in Computer Science Research, volume 93
2nd International Conference on Mathematics, Modeling and Simulation Technologies and Applications (MMSTA 2019)

Numerical Simulation of Flow Conditions of the Floating Channel in Shenzhen-Zhongshan Bridge Project

Hongming Chen[1,2], Shuhua Zhang[2] and Jie He[3]
[1]Key Laboratory of Coastal Disaster and Defence (Hohai University), Ministry of Education, Nanjing 210098, China
[2]College of Harbor, Coastal and Offshore Engineering, Hohai University, Nanjing 210098, China
[3]Nanjing Hydraulic Research Institute, Nanjing 210029, China

***Abstract*—In this paper, the two-dimensional water mathematical model of the Pearl River Estuary is established. Based on the verification of the hydrological data, the tidal current characteristics of the prefabricated immersed pipe pouring area and the floating channel are simulated, and the characteristics of the velocity fluctuation of the characteristic point are analyzed. The simulation results show that after the project is implemented, the tidal current velocity in the waters of the Longxue harbor basin is generally weak. The flow velocity of the basin in the Nansha Phase IV is relatively small, and the circulation in the water area of the mouth is weak, which provides favorable conditions for the anchorage of the platform; The maximum transverse flow is less than 1 mile/h, and the average value of the maximum transverse flow during the mid-tidal period is about 0.4 m/s; the maximum longitudinal outflow is now the AC and DE, and the maximum longitudinal flow during the neap tide period does not exceed 2 mile/h, and the navigation flow during the neap tide period. Conditions provide technical support for the location of the immersed pipe pouring area and the selection of the floating channel.**

Keywords—floating channel; transverse flow; longitudinal flow; numerical simulation

I. INTRODUCTION

Shenzhen-Zhongshan Bridge is a bridge connecting Shenzhen City and Zhongshan City, which spans Lingdingyang Estuary in the form of "bridge-island-tunnel". Lingdingyang Estuary has a complicated tidal process. When immersed tube sections and floating immersed tubes are prefabricated, due to the long operation window of floating, a high requirement is proposed for the current conditions of the channel. The maximum allowable transverse flow is 1 knot, while the maximum allowable longitudinal flow is 2 knots. Through mathematical modeling, the hydrologic characteristics and change rules of the floating channel over time were simulated, and the working window of immersed tube sections was calculated. Thus, it is fairly necessary to carry out a study on the numerical simulation of flow conditions of the floating channel from Longxue Harbor Basin to Shenzheng-Zhongshan Bridge.

According to relevant literature, so far many scholars have simulated the support transport of caisson sections through the floating channel, and studied the impact of the hydrologic environment of Lingdingyang Estuary. Feng Haibao [1] designed a floating channel for large immersed tubes in a limited water area, calculated key technical parameters of the channel, such as the width and depth, and applied them to the building of an immersed tube tunnel and an immersed tube floating channel for Hong Kong-Zhuhai-Macao Bridge. Ning Jinjin [2] came up with an approach that combined towing afore and towing alongside, for ultra-large immersed tubes by analyzing the channel limitations and complexity of ocean current conditions and gained a better control over the floating velocity and posture of immersed tubes through research and improvement. Ying Qiang et al. [3] analyzed the water and sediment conditions of the runoff of Lingdingyang Estuary, the tidal currents near the bridge and the characteristics of tidal levels and probed into the evolution characteristics and future development trend of shoals and troughs near the bridge. By initiating a physical model test on the tidal currents of Lingdingyang Estuary, Xu Qun [4] et al. believed that the influence scope and intensity of the construction of Hong Kong-Zhuhai-Macao Bridge on tidal dynamic environment was stronger near the East Artificial Island. He Jie et al. [5] simulated the hydrodynamic changes and impact degree on the Pearl River Estuary before and after the construction of the bridge, using a two-dimensional mathematical model of tidal current.

II. OVERVIEW OF THE WATERS

The tide type of Lingdingyang Estuary is irregular semidiurnal mixed tides. The tidal movement in Lingdingyang Estuary generally presents a trend of reciprocating, flooding in the north and ebbing in the south. The ebb currents are greater than flood currents. The average flood strengths in the east and west troughs are basically the same, while the ebb strength in the west trough is higher than that in the east trough. The Pearl River Estuary is a weak tide estuary, with a small tidal range. The average tidal range is 0.86m~1.69m, the maximum tidal range is 2.29~3.36m, the average flood strength is generally 0.4~0.5m/s and the average ebb strength is generally 0.5~0.6m/s. In the west trough, the flood current is strong, especially in dry seasons, while in the west trough, the ebb current dominates, especially for flood seasons. Whether at flood or ebb, the distribution of longitudinal flows in the estuary always gradually grows from the mouth to the head.

Fig. 1 shows an elliptic vector diagram of tides at various hydrologic stations during the flood seasons in recent years, H1, H2 and H3 were tide-gauge stations, stations V1, V2 and V3 were located in the water area along the immersed tube tunnel. Station V4 was located upstream of trial trough, and station V6 was located upstream of Aluminite Waterway. For all levels, the measured maximum flow rate always appeared in the surface layer of the ebb section at station V7 downstream of Aluminite Waterway. The maximum flow rate was 1.6m/s for spring tide, 1.4m/s for middle tide and 0.91m/s for neap tide. All of the stations basically presented the same rule: the flow rate of spring tides was the highest, followed by middle tide and neap tides. Ebb and flood currents basically presented a trend of reciprocating in the north-south direction.

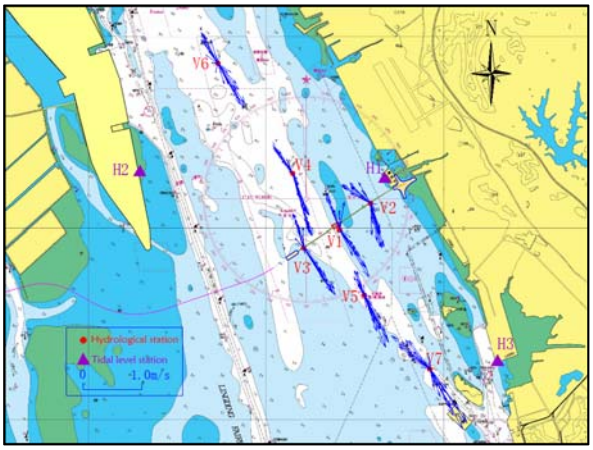

FIGURE I. LOCATIONS OF THE STATIONS AND THE ELLIPTIC VECTOR DISTRIBUTION OF MEASURED TIDES

III. GOVERNING EQUATION

When the size of plane is much larger then the vertical, two-dimensional shallow water equations can be used to describe the flow motion of calculated water area. Taking turbulence into account, flow governing equation can be expressed as formula:

$$\frac{\partial U}{\partial t}+\nabla E=S+\nabla E^{d}$$

with $U=(d,du,dv,ds)^{T}$, d is the total water depth, $d=h+\zeta$ （h is the water depth under horizontal plane.; ζ is the surface fluctuation）, $E=(F,G)$,and

$$F=\begin{pmatrix} du \\ du^{2}+gh^{2}/2 \\ duv \\ dus \end{pmatrix},\ G=\begin{pmatrix} dv \\ duv \\ dv^{2}+gh^{2}/2 \\ dvs \end{pmatrix},$$ where u and v are the velocity along the x and y coordinates, respectively. The turbulent diffusion of equation is expressed as: $E^{d}=(F^{d},G^{d})$

Where $F^{d}=\begin{pmatrix} 0 \\ \varepsilon_x d\partial u/\partial x \\ \varepsilon_x d\partial v/\partial x \\ K_x d\partial s/\partial x \end{pmatrix}$, $G^{d}=\begin{pmatrix} 0 \\ \varepsilon_y d\partial u/\partial y \\ \varepsilon_y d\partial v/\partial y \\ K_y d\partial s/\partial y \end{pmatrix}$,

and $\varepsilon_x, \varepsilon_y$ are the kinematic edd viscosity coefficients along the x and y coordinates, respectively, here isotropy is taken, then $E^{d}=(F^{d},G^{d})$, ε can be expressed as $\varepsilon=kdU_{*}$, the shear velocity can be expressed as $U_{*}=\frac{n\sqrt{g(u^{2}+v^{2})}}{d^{1/6}}$.

The source term S is written as formula:

$$S=S_0+S_f=\begin{pmatrix} 0 \\ S_{0x}+S_{fx}+fv \\ S_{0y}+S_{fy}-fu \\ -Fs \end{pmatrix}$$

where S_{ox} and S_{oy} are bed slopes along the x and y coordinates, respectively, $S_{0x}=-gd\,\partial z_b/x$, $S_{0y}=-gd\,\partial z_b/y$, z_b is the bottom level, and S_{fx} , S_{fy} are the friction losses in terms of the Manning's roughness coefficient n:

$$S_{fx}=-\frac{gn^{2}u\sqrt{u^{2}+v^{2}}}{d^{1/3}},\ S_{fy}=-\frac{gn^{2}v\sqrt{u^{2}+v^{2}}}{d^{1/3}},$$

The superscript f is Coriolis force, $f=2\omega\sin\Phi$, ω is the Earth's rotation speed, Φ is the geographical latitude.

IV. MESH GENERATION AND CALCULATION SCOPE

While carrying out a two-dimensional calculation on the tides of the estuary, given the characteristics of this area, that is, dense waterways, numerous islands, winding coastline and complex boundary, etc., the author used an unstructured grid to segment the computing domain The computing domain of the local mathematical model of the water area of floating channel is shown in Fig. 2. The sections of Xiaolan Waterway and Jiya Waterway at the entrance of Humen, the entrance of Jiaomen, Hongqimen and Hengmen were set as the upstream control sections. The downstream boundary was taken from a section from Zhuhai to Lantau Island in Hong Kong. The controlled water area of the model was about 3,000 km^2. The computing domain was divided into more than 100,000 triangular elements. The sea surface outside Lingdingyang Estuary was broad, so sparse and large-scale mesh generation was adopted. A mesh encryption was performed on the water areas along the main channels. The local model is shown in Fig. 3.

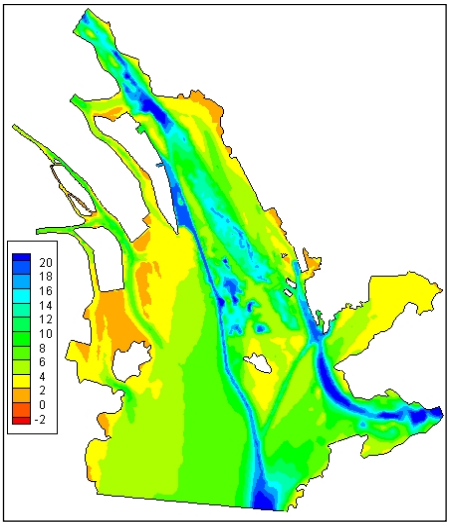

FIGURE II. CALCULATION RANGE OFTHE MATHEMATICAL MODEL

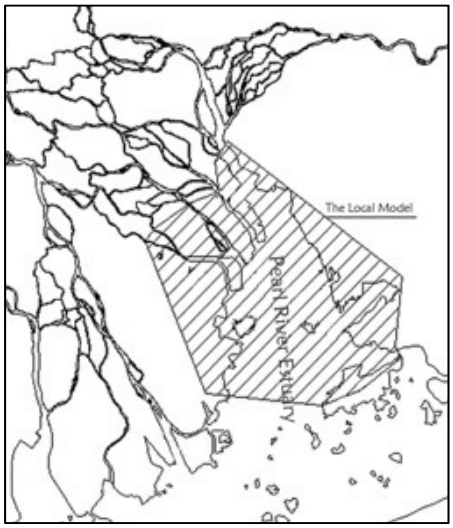

FIGURE III. THE LOCAL MODEL

V. ANALYSIS OF CALCULATION RESULTS

A. Analysis of the Flow Rates of Harbor Basin in the Casting Area

Harbor Basin under spring tides of flood seasons. Under the cover of surrounding shoals, the flow rates of tides in Longxue Harbor Basin were often weak. Point A01 was located in the waters of the casting areas and the flood strengths were generally greater than the ebb strengths. The average flood and ebb strengths at point A01 under spring tides of flood seasons were 0.44m/s and 0.11m/s respectively. Fig. 5, the ebb current along Wenchong Harbor Basin converged with the ebb current of Lingdingyang channel and flowed southward into the harbor basin in the 1st phase of Nansha Port. The flood current upstream of the 1st phase of Nansha Port was divided into two streams: one flowed to Wenchong Harbor Basin along the bank and the other entered the deep trough of Lingdingyang Estuary.

The flow rates of the harbor basin in the 4th phase of Nansha Port were generally small, and the circulating current at the entrance was weak. This offered favorable conditions for the harbor basin to be used as a typhoon anchorage. The flow rate in the intersection between the floating channel and Lingdingyang channel was high, and the angles between the main flood and ebb currents and the floating channel were large. For this reason, the transverse flow generated by the waters of the intersection was large.

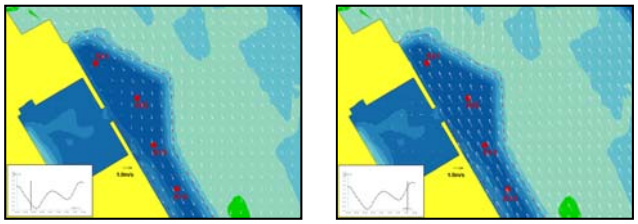

(A) EBB TIDE (B) FLOOD TIDE

FIGURE IV. PLANAR FLOW DISTRIBUTION OF LONGXUE HARBOR BASIN

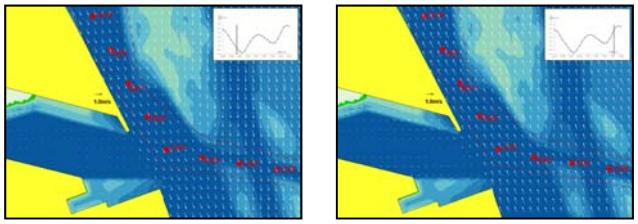

(A) EBB TIDE (B) FLOOD TIDE

FIGURE V. PLANAR FLOW DISTRIBUTION OF THE HARBOR BASIN IN THE 4TH PHASE OF NANSHA PORT

B. Flow Rates along the Channel

Fig. 6 gives the vector distribution of tides at various sections along the channel under spring tides of flood seasons, from which it can be seen that section AC was located in nearshore waters and the trends of voyage troughs were basically consistent with the flow directions of flood and ebb currents. The characteristic of flow rates along channel was that the flood currents were higher than ebb currents. The trends of the voyage troughs in sections CD and EF formed certain angles with the main tidal current. Section DE, which overlapped with Aluminite Waterway, was located in the main current area of Lingdingyang Estuary, the trends of voyage troughs were basically consistent with the flow directions of main flood and ebb currents, and ebb currents were greater than flood currents.

Under spring tides of flood seasons, the maximum flow rate was located at point A14 near Longxue Harbor Basin, being 1.17m/s. In section CD, the maximum ebb strength was located at point D01 of the turning section, being 1.10m/s. In section EF, the maximum flow rate was located at point E01 near the north end, being 0.72m/s. In both sections CD and EF, the maximum ebb strengths occurred at the turnings of the channel.

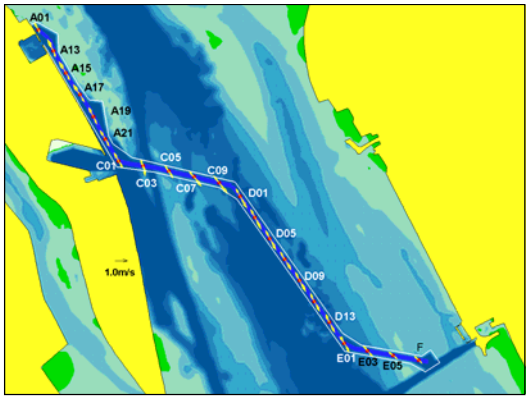

FIGURE VI. THE VECTOR DISTRIBUTION OF TIDES ALONG THE CHANNEL

C. Characteristic Flow Rates of the Channel

In the floating process of immersed tubes, a long working window was required. The maximum transverse flow should be less than 1 knot, while the maximum longitudinal flow should not exceed 2 knots. From Figs. 7-8, it can be seen that as the trends of voyage troughs in sections AC and DE were basically consistent with the flow directions of flood and ebb currents, the average of maximum transverse flow generated under different current conditions of flood seasons were small. There was no transverse flow whose flow rate was over 1 knot in a full tide process. In section CD, the average of maximum transverse flow was 0.52m/s, and the maximum transverse flow occurred at point C03 at the north end, with a flow rate of 0.73 m/s. The time required for a transverse flow whose flow rate was over 1 knot to occur in a full tide process was 7h. In section EF, the average of maximum transverse flow was 0.31m/s, and the maximum transverse flow occurred at point E01 at the north end, with a flow rate of 0.51m/s. The time required for a transverse flow whose flow rate was over 1 knot to occur in a full tide process was 2h. The longitudinal flows of voyage troughs, that is, up flows and down flows, whose flow rates were over 2 knots mainly occurred in section AC along Longxue Harbor Basin and section DE, which overlapped with Aluminite Waterway. But during middle and neap tides, the maximum longitudinal flows wouldn't exceed 2 knots. To sum up, the floating channel can satisfy the flow condition for navigation during neap tides.

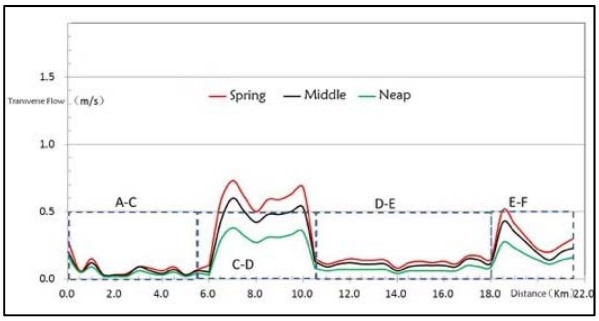

FIGURE VII. THE DISTRIBUTION OF MAXIMUM TRANSVERSE FLOWS ALONG THE FLOATING CHANNEL

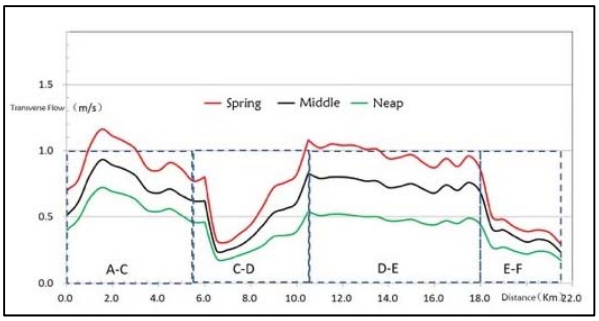

FIGURE VIII. THE DISTRIBUTION OF MAXIMUM LONGITUDINAL FLOWS ALONG THE FLOATING CHANNEL

VI. CONCLUSION

The measured data and the model test suggest that influenced by the underwater topography and nearshore boundary, the water area where the East Artificial Island is generally presents a trend of reciprocating, flooding in the north and ebbing in the south. The simulation results show that the trends of the voyage troughs in sections CD and EF form certain angles with main tidal currents, the maximum ebb strengths occur at the turning of the channel and the maximum transverse flow occurs in section CD. During neap tides, the maximum transverse flow is less than 1 knot. During middle tides, the average of maximum transverse flow is about 0.4m/s. The maxim longitudinal flows occur in sections AC and DE. During neap tides, the maxim longitudinal flow won't exceed 2 knots, that is, the flow condition for navigation during the neap tide.

REFERENCES

[1] FENG Hai-bao, SU Chang-xi.Design of immersed tube floating channel in limited water area[J]. Port and Waterway Engineering, 2018(01):200-204.

[2] NING Jin-jin, ZHENG Xiu-lei, SUN Jian, et al. Function analysis of tug's division on towing large tunnel element[J]. China HarbourEngineering, 2015(3): 67-69.

[3] YING Qiang, XIN Wen-jie, et al. An analysis of waterway processes near the Hong Kong-Zhuhai-Macao Bridge[J]. Hydro-Science And Engineering, 2012(2): 97-103.

[4] XU Qun, MO Si-ping, et al. Impacts of the Hong Kong-Zhuhai-Macao Bridge on flow environment of Lingdingyang estuary[J]. Hydro-Science and Engineering, 2012(2): 79-83.

[5] HE Jie, XIN Wen-jie, JIA Yu-shao. Numerical simulation of hydrodynamic impact of Hongkong Zhuhai Macao Bridge on Pearl River estuary[J]. Hydro-Science and Engineering, 2012(2) : 84-90.

[6] HE Jie, JIA Yu-shao, XIN Wen-jie. Study on the two-dimensional flow mathematical model of the Pearl River delta network and estuary[C]. Proceedings of the 18th China Ocean (Shore) Engineering Symposium. Beijing: China Ocean Pres, 2017.

[7] P. L. Roe. Approximate Riemann solvers, parameter vectors, and difference schemes [J]. Journal of Computational Physics, 1997, 135: 250-258.

[8] HE Jie, XIN Wen-jie. Numerical solution to the shallow water equation with diffusion motion[J]. Hydro−Science and Engineering, 2010(3) : 95−100.

[9] HE Jie, SUN Ying-jun, ZHAO Xin-sheng . Numerical model for hydrodynamic impact from HZM bridge[J]. Applied Mechanics and Materials, 2014, 580−583: 2146−2149.